The EMBO Journal vol.15 no.5 pp.999–1003, 1996

Multiple, coordinated Ca^{2+}-release events underlie the inositol trisphosphate-induced local Ca^{2+} spikes in mouse pancreatic acinar cells

Peter Thorn[1,2], Roger Moreton and Michael Berridge

The Laboratory of Molecular Signalling, Department of Zoology, Downing Street, Cambridge CB2 3EJ and [1]The Babraham Institute, Babraham, Cambridge CB2 4AT, UK

[2]Corresponding author

Ca^{2+} wave initiation and non-propagating Ca^{2+} spikes occur as a result of localized Ca^{2+} release from the more sensitive intracellular Ca^{2+} stores. Using high spatial and temporal Ca^{2+}-imaging techniques we have investigated inositol 1,4,5 triphosphate ($InsP_3$)-induced local Ca^{2+} spiking, which occurs at the site of Ca^{2+} wave initiation in pancreatic acinar cells. The spatial and temporal organization of a single spike suggested discrete hot spots of Ca^{2+} release. Further analysis of long trains of Ca^{2+} spikes demonstrated that these hot spots showed regenerative Ca^{2+}-release events which were consistently active from spike to spike. Regions adjacent to these hot spots also showed regenerative Ca^{2+}-release events of similar amplitude but with a much lower frequency of occurrence. We conclude that the $InsP_3$-induced non-propagating Ca^{2+} spikes can be devolved into smaller components of release. Our results are consistent with a model of coordinated activity of pacemaker hot spots of Ca^{2+} release that recruit and entrain active Ca^{2+}-release events from surrounding regions.

Keywords: calcium signalling/$InsP_3$/pancreatic acinar cells

Introduction

Inositol 1,4,5 trisphosphate ($InsP_3$)-dependent release from intracellular Ca^{2+} stores is a ubiquitous process that underlies many physiological functions. In many cells Ca^{2+} release is initiated at a single site and then spreads as a wave across the cell (Berridge, 1993). In *Xenopus* oocytes it has recently been shown that low levels of $InsP_3$ elicit repetitive spikes of Ca^{2+} (called puffs) which, at higher stimulus levels, subsequently lead to propagated waves (Yao *et al.*, 1995). Therefore, each puff represents an initiation site for a Ca^{2+} wave and is a spatially discrete entity calculated to arise from the coordinated opening of a small number of $InsP_3$ receptors (Yao *et al.*, 1995). Pancreatic acinar cells have also provided valuable insights into the process of wave initiation (Kasai and Augustine, 1990; Petersen, 1992; Kasai *et al.*, 1993; Thorn *et al.*, 1993, 1994) and propagation (Nathanson *et al.*, 1992) in mammalian cells. With low levels of agonist stimulation or stimulation via the injection of $InsP_3$, repetitive non-propagating spikes of Ca^{2+} release, spatially restricted to the wave initiation site (the secretory pole), are observed in acinar cells (Kasai *et al.*, 1993; Thorn *et al.*, 1993). These local oscillations peak at a Ca^{2+} concentration of ~150 nM, have a duration of 2 s and are independent of extracellular Ca^{2+} (Wakui *et al.*, 1989; Thorn *et al.*, 1993). However, beyond this basic level of analysis very little is known of the Ca^{2+} signal characteristics.

In this study we have investigated the Ca^{2+}-release events associated with the non-propagating $InsP_3$-induced local spikes in pancreatic acinar cells. The data provide the most detailed analysis of the spatial aspects of $InsP_3$-evoked Ca^{2+} release in mammalian cells to date. The results demonstrate spatial inhomogeneities of Ca^{2+} release within the secretory pole region which indicate that each Ca^{2+} spike is due to the coordinated action of multiple, spatially discrete, release events. We conclude that pacemaker regions with a high frequency of occurrence of Ca^{2+}-release events act to entrain active Ca^{2+} release from surrounding regions.

Results

Spatial inhomogeneity of the Ca^{2+} spike

Trains of Ca^{2+} spikes, spatially localized to the secretory pole, were elicited in mouse pancreatic acinar cells, stimulated by low concentrations of $InsP_3$. In a total of 52 cells, we used the technique of whole-cell patch-clamp and simultaneous single-cell Ca^{2+} imaging of Fura-2 fluorescence to investigate the spatial and temporal characteristics of these repetitive spikes. The technique of loading Fura-2-free acid directly into the cells, via the solution of the patch pipette, reports changes in cytosolic Ca^{2+} without contamination by fluorescence from intracellular organelles. Figure 1A shows a pseudocolour representation of a single spike induced by the infusion of 15 μM $Ins(2,4,5)P_3$ through the patch pipette. Thirty one ratio images were collected every 80 ms over the duration of a control period and during the Ca^{2+} spike, and each series was averaged to produce Figure 1A and B. The figure illustrates the spatially restricted nature of the Ca^{2+} spike in that areas of elevated Ca^{2+} are limited to the secretory pole region of the cell (identified under bright field illumination by the clustering of the dark zymogen granules). Within the secretory pole the Ca^{2+} signal is heterogeneous with spatially discrete hot spots of Ca^{2+} elevation. Under control conditions with no $InsP_3$ or with co-injection of $InsP_3$ and heparin (n = 9), no Ca^{2+} responses were observed.

Temporal characteristics of the Ca^{2+} spike

When a small grid was positioned over a region of hot spots and sampled at a rate of 10 Hz, a series of discrete spikes was recorded and averaged (Figure 2). The graph, obtained by averaging the data from 11 consecutive spikes, shows an asymmetric response with a rapid rise time to

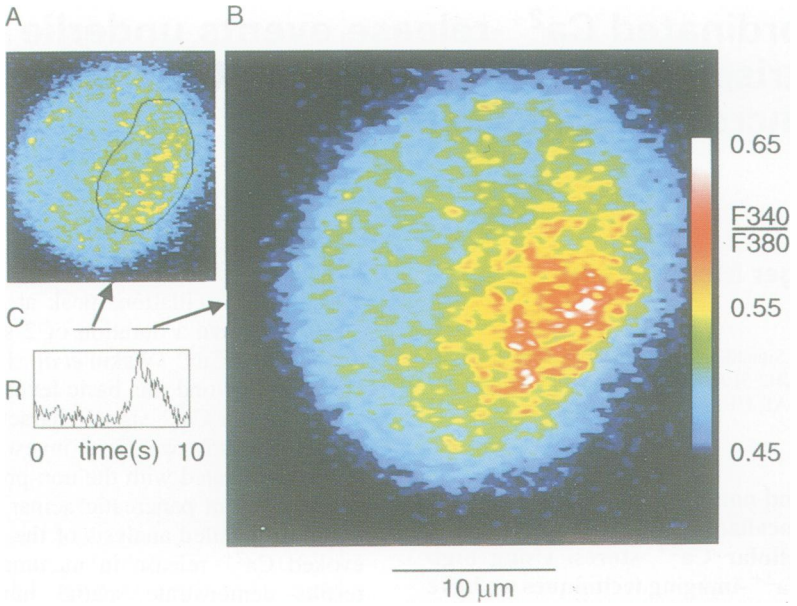

Fig. 1. Ca^{2+}-spike response of a single pancreatic acinar cell infused with 15 μM Ins(2,4,5)P_3. A pseudocolour representation of the average Ca^{2+} changes from 31 images before (**A**) and 31 images during one single spike (**B**) which was part of a record of a train of spikes induced by Ins(2,4,5)P_3. The average Ca^{2+} response within the secretory pole (see black line on control pseudocolour image) is illustrated [within the rectangle, (**C**)] along with bars showing the position in the record where the control and test images were obtained. The overall Ca^{2+} rise within the secretory pole during the spike is punctuated by small areas of local Ca^{2+} hot spots.

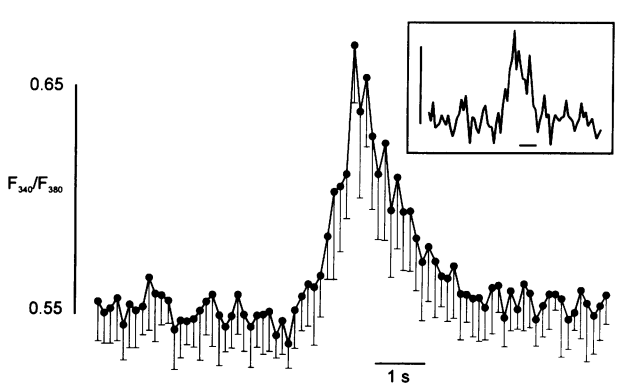

Fig. 2. Temporal analysis of local Ins(2,4,5)P_3-induced Ca^{2+} spikes. The mean and standard error of the Ca^{2+} signal obtained over 11 consecutive Ca^{2+} spikes from a 16 μm^2 area centred over one of the Ca^{2+} hot spots in the same cell as in Figure 1. The peak of each spike was used to align the average. An inset shows that each single spike showed the complex rising phase.

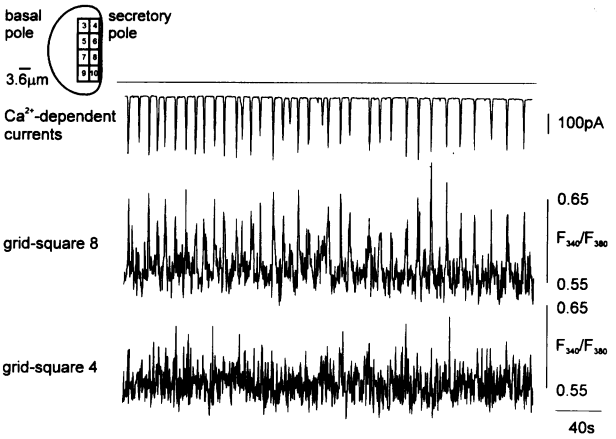

Fig. 3. Whole cell and Ca^{2+} recording of the Ca^{2+}-dependent currents and the Ca^{2+} signal in two areas within the secretory pole. The cell was stimulated with 15 μM Ins(2,4,5)P_3. The cartoon in the upper left corner illustrates the position and size of the grid over the secretory pole from which the Ca^{2+} signals were recorded. The upper trace shows the Ca^{2+}-dependent current trace recorded under voltage clamp at a membrane potential of –30 mV. The solid line above shows the 0 current level. Under these conditions the current is composed of both the Ca^{2+}-dependent Cl^- and non-selective cation channels. The middle trace is the average Ca^{2+} signal recorded from the area defined as grid-square 8. The Ca^{2+} signal from grid-square 4 is shown in the lower trace.

a peak of Ca^{2+} within 1.2 s and a slower decay which was adequately fitted to a single exponential with a time constant of 1.08 s. At this sampling rate the rising phase of the Ca^{2+} spike was not well resolved. However, in all the spikes analysed it was apparent that the rising phase was not monotonic but rather, was composed of two or more steps (see inset of a single spike, Figure 2).

Localization of active sites of Ca^{2+} release

The spatial inhomogeneities shown in Figure 1 and the complex rising phase of the spike shown in Figure 2 suggest that multiple, spatially separate, release events may occur during the Ca^{2+} spike. To investigate this further, we utilized long duration recordings of trains of Ca^{2+} spikes. Upon infusing the cell with 15 μM $InsP_3$, a train of spikes in the whole-cell Ca^{2+}-dependent current (Figure 3, upper trace) was recorded. Simultaneously, the average Ca^{2+} concentration was measured within 4×4 μm grids located over the secretory pole of a single pancreatic acinar cell. Although spike frequency gradually decreased during the course of this trace, the size and shape of each spike did not change appreciably, indicating a stable mechanism of spike generation. Two examples of the average Ca^{2+} responses recorded from two separate grid-squares over the secretory pole are shown in Figure 3 (lower traces). The Ca^{2+} response of grid-square 8 shows

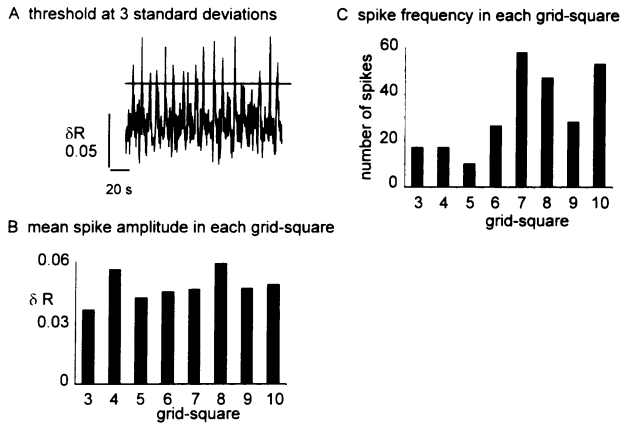

Fig. 4. A detailed analysis of the Ca^{2+} spikes in the different grids across the secretory pole. (**A**) shows an example of the threshold analysis used to identify the spikes. In this analysis a segment of the recording, where no spike activity was observed either in the current or in the Ca^{2+} signal, was used to estimate the standard deviation of the fluorescence noise. A running average of 30 points was applied to the raw data, sufficient to minimize the effect of the Ca^{2+} spikes and provide a measure of slow baseline fluctuations. A criteria of three times the standard deviation of the noise was chosen, any signal above this threshold being taken as a spike event. To apply this threshold we added the measure of three standard deviations of the noise to the smoothed measure of the signal baseline for each grid-square. The result of this analysis is shown in (A) and was used in all subsequent experiments. (**B**) shows a plot of the mean amplitude of the spikes in each grid-square. The amplitude of the spikes in grid-square 3 were significantly smaller; this may be because this area is right at the edge of the secretory pole and may encompass part of the unresponsive basal pole. (**C**) shows a plot of spike frequency for each of the grid-squares.

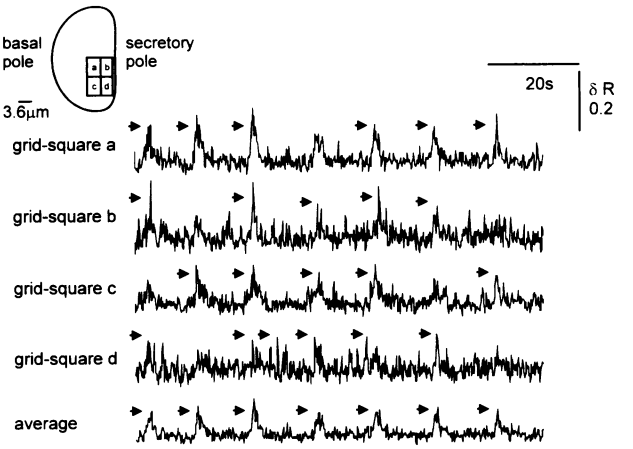

Fig. 5. Spatio-temporal variations in excitability analysed at greater resolution. A cartoon representation shows the dimensions and position of the grid used in this analysis. Ca^{2+} traces from the grid-squares are shown and those events that were identified as Ca^{2+} spikes, on the basis of the threshold of three standard deviations greater than the noise, are indicated by an arrow. Also shown is the overall Ca^{2+} signal recorded in all the grid-squares (bottom trace). Only at the third and fifth average spike is a discrete Ca^{2+} spike observed in all grid-squares.

repetitive Ca^{2+} spikes which, at this sampling rate, occur in register with the Ca^{2+}-dependent current trace. In contrast, the Ca^{2+} response from grid-square 4, which is still within the secretory pole, shows low-frequency Ca^{2+} spikes which were of similar amplitude to those of grid-square 8. Although of much lower frequency, the spikes observed in grid-square 4 were generally either coincident with or slightly delayed from those of grid-square 8.

Criteria for accepting an event as a Ca^{2+} spike

To further the analysis we need a reliable method of identifying Ca^{2+} spikes above the background noise. Ideally this would be derived from measurements of the fluorescence noise level in control cells not injected with $InsP_3$ or injected with heparin to block the $InsP_3$ receptor. However, measurements on nine different cells under such conditions failed to produce comparable results because of the variability in Fura-2 filling from cell to cell. Instead, the fluorescence noise for each experimental cell was estimated from a period during the interspike interval and empirically all points lying more than three standard deviations of the noise above the mean baseline were accepted as spike events (see Figure 4A). Using this method we identified Ca^{2+} spikes and obtained figures for the amplitude and frequency of spiking within grid-squares in five different cells.

Higher resolution analysis of the Ca^{2+} signals during a train of spikes

Mean spike Ca^{2+} amplitudes in each grid-square are shown in Figure 4B. The small variation in amplitude from grid-square to grid-square was thought to be the result of Ca^{2+}-release events occurring in and just out of the plane of focus. However, using this analysis we were unable to rule out genuine small differences in amplitude in different grid-squares. In contrast to the roughly similar amplitudes, Figure 4C illustrates a wide variability in frequency of spikes in each of the grid-squares. These data indicate grid-squares 7, 8 and 10 as having a greater spike frequency than other regions.

To investigate the Ca^{2+} spikes more closely, the same cell used in Figures 3 and 4 was re-analysed at greater temporal resolution using grid-squares over a region previously identified as a hot spot (Figure 5). The sampling rate was 10 Hz and individual events of a greater amplitude than the three standard deviations of the noise were identified as spikes (arrows on Figure 5). There are a number of important points that are revealed by this analysis. First, all grid-squares show responses with rapid rise times which are characteristic of regenerative responses rather than passive Ca^{2+} diffusion from a single point source. Secondly, in every grid-square occasional failures to spike support the idea that the spike events in each grid-square are regenerative. Thirdly, even in adjacent grid-squares the Ca^{2+} response can be very different. For example, the final spike in grid-square a is not observed in the adjacent grid-square b. This indicates that the areas of the grid-squares fully encompass local Ca^{2+}-release events. Fourthly, although spike-like events are not always seen in each grid-square, when they do occur they are loosely coordinated (within 200 ms) across more than one grid-square.

The results also show that each average Ca^{2+} spike (lower trace) is composed of a different pattern of discrete Ca^{2+}-release events. Grid-square a consistently shows a regenerative response for all but one of the average Ca^{2+} spikes. However, responses in other regions are seen in some average Ca^{2+} spikes but not in others. The results provide strong evidence for patterns of local Ca^{2+} release which become coordinated to produce the macro event of

the average Ca^{2+} spike in the whole region of the secretory pole.

Discussion

Our experiments describe the spatio-temporal characteristics of the $InsP_3$-induced local Ca^{2+} spikes in mouse pancreatic acinar cells. The data are consistent with the idea that the secretory pole responds to low levels of $InsP_3$ by becoming an excitable medium capable of generating repetitive Ca^{2+} spikes. For the first time, we demonstrate that this response can be devolved into smaller spatially discrete components of Ca^{2+} release which are coordinated to form the spike. Recording trains of local Ca^{2+} spikes over an extended period of time allowed us to identify regional hot spots of Ca^{2+} release which were consistently active at almost every spike. In contrast, other regions showed only occasional Ca^{2+}-release events which were nevertheless temporally coordinated across the secretory pole. These regional differences in Ca^{2+} responsiveness are not consistent with a model of the local Ca^{2+} spike, where a single region of active release is surrounded by regions that only pick up a passive spread of Ca^{2+}. Instead, discrete regions of Ca^{2+} release appear to act as pacemakers entraining active release from surrounding regions.

Spatial organization of the signal

The data presented in Figure 4 support the idea that within each of the grid-squares, local Ca^{2+}-release mechanisms exist which are capable of providing discrete regenerative responses. In previous work, the secretory pole was shown to have a higher sensitivity for Ca^{2+} release compared with the basal pole (Thorn *et al.*, 1993). It was proposed that this may be due to a clustering of $InsP_3$ receptors either at a higher density or with a higher affinity for $InsP_3$ in this pole of the cell (Thorn *et al.*, 1993). The analysis presented here allows us to isolate local differences in the Ca^{2+} signals within the secretory pole. These may also be due to inhomogeneities in the properties or density of the $InsP_3$ receptor. An additional factor may be a differential distribution of Ca^{2+}-ATPases leading to more efficient, local Ca^{2+}-uptake mechanisms that rapidly refill the stores and increase the frequency of spiking (Camacho and Lechleiter 1993; Petersen *et al.*, 1993).

A single region of 5–10 μm diameter, the trigger zone, within the secretory pole of rat pancreatic acinar cells has been identified by Kasai *et al.* (1993) as the origin of a global Ca^{2+} response. This is probably analogous to the sensitive area we have identified, although our study of trains of spikes shows, for the first time, that the heterogeneity of response within the secretory pole occurs not only spatially but can also vary from spike to spike. A similar observation of coordinated Ca^{2+} signals has also been made from adjacent release sites in *Xenopus* oocytes (Yao *et al.*, 1995). A potential candidate for this coordination could be diffusional spread of Ca^{2+} released into the cytosol. In this way, an initial release of Ca^{2+} would raise the cytosolic Ca^{2+} and sensitize the surrounding $InsP_3$ receptors. Certainly, cytosolic Ca^{2+} buffering is crucial to the local Ca^{2+} spike which can be abolished by Fura-2 concentrations in the pipette above 200 μM or by perfusion of low concentrations of BAPTA-AM in the bathing solution (unpublished observations). However, we cannot rule out additional factors that may act to coordinate the release of Ca^{2+} across the regions of the secretory pole.

Relationship to quantal release

Quantal Ca^{2+} release is normally used to refer to the property of fractional release of Ca^{2+} from intracellular stores in response to submaximal stimulation (Muallem *et al.*, 1989). The amount of Ca^{2+} released is proportional to the stimulus and reaches a plateau, either as the result of the balance of mechanisms of release and re-uptake (van de Put *et al.*, 1994) or as an intrinsic inactivation of the release mechanism. One interpretation of these experimental findings is that there is a heterogeneity in the sensitivity of Ca^{2+} stores (Bootman *et al.*, 1994). The results presented in this paper are consistent with microregional heterogeneities in Ca^{2+} store sensitivity.

Relationship with other local Ca^{2+} responses

Spatially restricted Ca^{2+}-release events which do not trigger a global Ca^{2+} response have now been described in a number of cell types. Discrete Ca^{2+} sparks have been observed in cardiac (Cheung *et al.*, 1993) and smooth muscle (Nelson *et al.*, 1995), which are thought to be due to openings of small clusters of ryanodine receptors. The local Ca^{2+} responses in pancreatic acinar cells resemble the local Ca^{2+} puffs in *Xenopus* oocytes (Yao *et al.*, 1995) in that they are activated by low levels of $InsP_3$, have similar firing frequencies, amplitude, shapes and also encompass a similar area. Based on calculations of puff density in the oocyte (1/30 μm^2), only one puff would be found in the secretory pole of pancreatic acinar cells. However, the kinetics of the oocyte puff are much faster than the local acinar cell spike and show a rapid rise, peaking at 100 ms, and a decay over 300–400 ms. The slower kinetics of the local Ca^{2+} spike in the acinar cells can now be explained by a sequential recruitment of the spatially separate smaller release units described in this paper.

Physiological significance of the discrete events

An additional observation from our data is the almost perfect synchronization between the Ca^{2+} response in a single grid-square and the Ca^{2+}-dependent current response (see Figure 3, grid-square 8). This strongly suggests a very close physical proximity between this site of Ca^{2+} release and the Ca^{2+}-dependent channels in the plasma membrane. The channels are known to be important in fluid secretion and our data highlight the physiological significance of these discrete Ca^{2+}-release events. A very similar link has been drawn in smooth muscle cells between sparks of Ca^{2+} release from ryanodine receptors which activate Ca^{2+}-dependent K^+ channels, leading to membrane hyperpolarization and muscle relaxation (Nelson *et al.*, 1995).

Materials and methods

Whole-cell patch-clamp techniques were employed (Hamill *et al.*, 1981) on single, acutely isolated pancreatic acinar cells (Thorn *et al.*, 1994). All experiments were carried out at room temperature (2–22°C). Pipettes of 2–5 MΩ were pulled (Narashige pipette puller, Japan) and cells were voltage-clamped at a membrane potential of –30 mV (Biologic patch clamp amplifier, France). Cells with a series resistance of greater than

three times the pipette resistance were rejected. The pipette solution contained (mM): 140 KCl, 1 $MgCl_2$, 10 HEPES, 2 ATP, pH 7.2 with KOH and 100–200 μM Fura-2-free acid (Molecular Probes, USA). The bath solution contained (mM) 135 NaCl, 5 KCl, 1 $MgCl_2$, 1 $CaCl_2$, 10 HEPES pH 7.4 with NaOH. Ins(2,4,5)P_3 was a gift from Dr Robin Irvine (Babraham Institute, Cambridge, UK) and was included in the pipette solution at 5–15 μM. Heparin (Low molecular weight, Sigma, UK) 500 μg/ml was included in the pipette solution in some control experiments. The cytosolic Ca^{2+} signal was recorded using Fura-2 fluorescence on a Ca^{2+}-imaging machine built around a Nikon inverting microscope (Japan), 100× objective 1.3 na; excitation using a dual micrometer Xenon light source set at 340 and 380 nM; detection of emitted light using a Photonic Science extended ISIS camera (UK) and data were collected and analysed with Synoptics hardware (UK) and custom software (Cheek *et al.*, 1993). All Ca^{2+} changes were expressed as the ratio (R) of emission at the excitation wavelengths of 340/380 nm.

Acknowledgements

We would like to thank Dr Tim Cheek (Zoology Department, Cambridge, UK) for help throughout this project, and Professor Fred Fay (University of Massachusetts, USA) and Dr David Brown (The Babraham Institute, Cambridge, UK) for discussion and analysis. Peter Thorn is supported by a Senior Babraham Research Fellowship.

References

Berridge,M.J. (1993) Inositol trisphosphate and calcium signalling. *Nature*, **361**, 315–325.

Bootman,M.D., Cheek,T.R., Moreton,R.B., Bennett,D.L. and Berridge, M.J. (1994) Smoothly graded Ca^{2+} release from inositol 1,4,5-trisphosphate-sensitive Ca^{2+} stores. *J. Biol. Chem.*, **269**, 24783–24791.

Camacho,P. and Lechleiter,J.D. (1993) Increased frequency of calcium waves in *Xenopus laevis* oocytes that express a calcium-ATPase. *Science*, **260**, 226–229.

Cheek,T.R., Morgan,A., O'Sullivan,A.J., Moreton,R.B., Berridge,M.J. and Burgoyne,R.D. (1993) Spatial localization of agonist-induced Ca^{2+} entry in bovine adrenal chromaffin cells: different patterns induced by histamine and angiotensin II and relationship to catecholamine release. *J. Cell Sci.*, **109**, 913–921.

Cheung,H., Lederer,W.J. and Cannell,M.B. (1993) Calcium sparks: elementary events underlying excitation-contraction coupling in heart muscle. *Science*, **262**, 740–744.

Hamill,O.P., Marty,A., Neher,E., Sakmann,B. and Sigworth,F.J. (1981) Improved patch clamp techniques for high resolution current recording from cells and cell-free membrane patches. *Pflugers Arch.*, **391**, 85–100.

Kasai,H. and Augustine,G.J. (1990) Cytosolic Ca^{2+} gradients triggering unidirectional fluid secretion from exocrine pancreas. *Nature*, **348**, 735–738.

Kasai,H., Li,Y.X. and Machete,Y. (1993) Subcellular distribution of Ca^{2+} release channels underlying Ca^{2+} waves and oscillations in exocrine pancreas. *Cell*, **74**, 669–667.

Muallem,S., Pandol,S.J. and Beeker,T.G. (1989) Hormone-evoked calcium release from intracellular stores is a quantal process. *J. Biol. Chem.*, **246**, 205–212.

Nathanson,M.H., Padfield,P.J., O'Sullivan,A.J., Burgstahler,A.D. and Jamieson,J.D. (1992) Mechanisms of Ca^{2+} wave propagation in pancreatic acinar cells. *J. Biol. Chem.*, **267**, 18118–18121.

Nelson,M.T., Cheng,H., Rubart,M., Santana,L.F., Bonev,A., Knot,A. and Lederer,W.J. (1995) Relaxation of arterial smooth muscle by calcium sparks. *Science*, **270**, 633–637.

Petersen,O.H. (1992) Stimulus secretion coupling: cytoplasmic calcium signals and control of ion channels in exocrine acinar cells. *J. Physiol.*, **448**, 1–51.

Petersen,C.C.H., Petersen,O.H. and Berridge,M.J. (1993) The role of endoplasmic reticulum calcium pumps during cytosolic calcium spiking in pancreatic acinar cells. *J. Biol. Chem.*, **268**, 22262–22264.

Thorn,P., Lawrie,A., Smith,P.M., Gallacher,D.V. and Petersen,O.H. (1993) Local and global cytosolic Ca^{2+} oscillations in exocrine cells evoked by agonists and inositol trisphosphate. *Cell*, **74**, 661–668.

Thorn,P., Gerasimenko,O. and Petersen,O.H. (1994) Cyclic ADP ribose regulation of ryanodine receptors involved in agonist evoked cytosolic Ca^{2+} oscillations in pancreatic acinar cells. *EMBO J.*, **13**, 2038–2043.

Van de Put,F.H.M., De Pont,J.J.H.H.M and Willems,P.H.G.M. (1994) Heterogeneity between intracellular Ca^{2+} stores as the underlying principle of quantal Ca^{2+} release by inositol 1,4,5-trisphosphate in permeabilized pancreatic acinar cells. *J. Biol. Chem.*, **269**, 12438–12443.

Wakui,M., Potter,B.V.L. and Petersen,O.H. (1989) Pulsatile intracellular calcium release does not depend on fluctuations in inositol trisphosphate concentration. *Nature*, **339**, 317–320.

Yao,Y., Choi,J. and Parker,I. (1995) Quantal puffs of intracellular Ca^{2+} evoked by inositol trisphosphate in *Xenopus* oocytes. *J. Physiol.*, **482.3**, 533–553.

Received on October 13, 1995; revised on November 1, 1995